Enhanced continuum poromechanics to account for adsorption induced swelling of saturated isotropic microporous materials

Romain Vermorel, Gilles Pijaudier-Cabot

Enhanced continuum poromechanics to account for adsorption induced swelling of saturated isotropic microporous materials

R. Vermorel[a,*], G. Pijaudier-Cabot[a]

[a]*Laboratoire des Fluides Complexes et leurs Réservoirs (UMR 5150), Université de Pau et des Pays de l'Adour, Allée du Parc Montaury, F-64600 Anglet*

Abstract

Poromechanics offers a consistent theoretical framework for describing the mechanical response of porous solids fully or partially saturated with a fluid phase. When dealing with fully saturated microporous materials, which exhibit pores of the nanometer size, effects due to adsorption and confinement of the fluid molecules in the smallest pores must be accounted for. From the mechanical point of view, these phenomena result into volumetric deformations of the porous solid, the so-called "swelling" phenomenon. The present work investigates how the poromechanical theory may be refined in order to describe such adsorption and confinement induced effects in microporous solids. Poromechanics is revisited in the context of isotropic microporous materials with generic pore size distributions. The new formulation introduces an effective pore pressure, defined as a thermodynamic variable at the representative volume element scale (mesoscale), which is related to the overall mechanical work of the confined fluid. Accounting for the thermodynamic equilibrium of the system, we demonstrate that the effective pore pressure depends on macroscopic variables, such as the bulk fluid pressure, the temperature and the total and excess adsorbed quantity of fluid. As an illustrating example, we apply the model to compute strains and variations of porosity in the case of the methane and carbon dioxide sorption on coal. Agreement with experimental data found in the literature is observed.

Keywords: poromechanics, microporosity, swelling, adsorption, fluid confinement, microporous solids, micropores, coal, carbon

1. Introduction

Poromechanics offers a consistent theoretical framework for describing the mechanical response of porous solids saturated, or partially saturated with a fluid phase. The theory is based upon the superposition of the solid and liquid phases. In the case of fully saturated porous solids, it is assumed that the fluid-solid interaction is restricted to the influence of the pressure on the inner surface of the porous material. In partially saturated porous solids,

*Corresponding author
Email address: romain.vermorel@univ-pau.fr (R. Vermorel)

additional forces, i.e. capillary forces are introduced. Many authors have used this modern theoretical framework, which is thoroughly described in the textbooks by Coussy [1, 2] and need to be adapted in the case of microporous solids.

As "isotropic microporous" materials, we refer to amorphous solids which contain pores of size less than 2 nm exclusively, consistent with the IUPAC classification. For instance, manufactured disordered porous carbons fits that definition. Furthermore, numerous multi-scale disordered porous materials, such as coal, cement paste or tight rocks, exhibit significant microporosity. As a consequence, the proper description of the mechanical response of the microporous part of these materials is of great importance in the context of chemical engineering processes, building construction, fossil fuels production and geological storage. Aside from the classical fluid-solid interaction observed in macroporous materials, there are additional effects that should be considered in the case of micropores filled with a fluid phase. Two features should be distinguished: adsorption and fluid confinement (or molecular packing): (i) adsorption takes place at the inner surface of the pores; (ii) the fluid is confined and a single fluid molecule can interact with all the atoms of the pore surface. As a result, interactions between molecules of the fluid and the solid are modified, it cannot develop in the same way as if the fluid would be placed in a large container. This effect includes fluid-fluid and fluid-solid interactions. From the mechanical point of view, these phenomena result into volumetric deformations of the porous solid. Swelling is commonly observed during sorption-desorption of several gases such as carbon dioxide (CO_2) or methane (CH_4) in charcoal, see e.g. the papers by Levine [3], Day et al [4, 5] and Ottiger et al [6], although seminal experimental works of Meehan [7] and Bangham and Fakhroury [8] date back to the 1920s.

CO2 swelling of coal and carbon absorbents has been investigated within the framework of poromechanics. Vandamme et al [9] extended poromechanics to surface effects adding energy stored at the solid-fluid interface in the formulation. However, the interaction stresses are restricted to surface adsorption effects, which is suitable for mesoporous materials only. Following a comparable approach, Pan and Connell [10] proposed an analytical model to compute adsorption induced swelling of coal. Assuming a cylindrical pore geometry, they introduced a surface stress at the the pore walls which is related to a Langmuir adsorption model. The Langmuir model parameters and the poromechanical properties are then fitted to adsorption and swelling data respectively. Although the fitted theoretical curves match well the experimental results, the model requires the adjustment of interstitial fluid properties, of which consistency remains difficult to assess. Mushrif and Rey [11] followed some similar reasoning as far as the poromechanics formulation is concerned. They computed the adsorption-induced strain directly from the chemical potential of the adsorbate, more specifically from the difference between the chemical potential of the fluid in the strained and unstrained absorbent. Good agreement with swelling data on activated carbon particles was observed. Recently, Brochard et al [12, 13] proposed a sound reformulation of poromechanics to account for adsorption induced strains in saturated microporous solids. The model derives constitutive equations from the free energy balance of the open system composed of the solid skeleton and the interstitial fluid, instead of the free energy balance of the porous skeleton only, as in standard poromechanics. Although the theory is laid down

in very general perspectives, it requires further assumptions, or alternatively the help of molecular simulations, for the model to be applicable. The molecular simulations performed on a model porous carbon agree well with experimental data found in the literature [6].

Apart from the global volumetric expansion, the porosity of the microporous material is likely to significantly increase upon sorption. Accounting for this effect is important for the estimation of the quantity of fluid stored in the microporous solid. Furthermore, because of the influence of pores constrictions[14], the description of the variation of porosity is also important in the prospect of modeling the fluid transport properties of the material. In the approaches discussed above, although the predictions of the swelling strains are satisfying, the direct description of the variation of microporosity upon swelling of the material is left unspecified. This probably comes from the difficulty of defining the stress exerted by the interstitial fluid on the solid phase. For the sake of understanding this issue, let us consider a saturated microporous solid placed in a container filled with a fluid at a bulk pressure (bulk solution). According to molecular simulations of adsorption in single slit pores, the pressure inside the pores is different from the bulk pressure as a result of adsorption and confinement [15]. This difference can amount to one or two orders of magnitude for very small pores ($\leq 1\,\mathrm{nm}$). Furthermore, this difference should depend on the bulk pressure, on the temperature, and on the pore sizes and geometry. In a solid with a complex microporous structure, inner stresses are different from one pore to another and different from the bulk pressure, if the pores are sufficiently small. As a result, the direct upscaling of these effects from the local pore scale to the macro-scale seems intractable when dealing with isotropic disordered microporous solids. The proper description of the variation of microporosity therefore requires some alternative approach.

In this paper, we investigate how the poromechanical theory may be refined to account for fluid confinement effects in the micropores, without the need of any pore scale modeling. The new formulation introduces an effective pore pressure as a thermodynamical variable defined at the representative volume element scale (mesoscale), which accounts for the overall mechanical work produced by the confined fluid filling the microporosity. Furthermore, we refer to the thermodynamic equilibrium condition of the system composed of the microporous skeleton, the interstitial and external bulk reference fluids. By doing so, we derive a relation between the effective pore pressure and macroscopic quantities such as the temperature, the bulk fluid pressure and the total and excess adsorbed mass of fluid. In isothermal conditions, the theory predicts an effective pore pressure larger than the external bulk pressure. Assuming a poroelastic behavior of the material, this results into a volumetric dilation of the porous skeleton consistent with the swelling phenomenon. As an illustrating example, we calculate the swelling strain and variation of porosity in the case of methane and carbon dioxide sorption on coals. Comparison with coal swelling data found in the literature is satisfactory.

2. Extension of poromechanics to the case of saturated isotropic microporous solids

In this section, we extend continuum poromechanics to the case of isotropic microporous solids saturated by a fluid phase. After introducing the general notations, we define an effective pore pressure that averages the effects of fluid adsorption and confinement in the micropores to the mesoscale at which continuum modeling becomes relevant. Then, referring to the principle of thermodynamical equilibrium, we derive a constitutive equation for the effective pore pressure and discuss its effect on macroscopic volumetric strains.

2.1. Nomenclature and definitions

The porous medium is viewed as an open thermodynamic system, which consists in the superposition of a porous solid phase, the skeleton, and an interstitial fluid phase which can exchange fluid mass with an external reference bulk solution. Hence, we use subscripts s or f to refer to a variable related to the skeleton or the interstitial fluid respectively. Moreover, the subscript b will be used when referring to the bulk solution. Indeed, because of adsorption and confinement effects, it is essential to distinguish the interstitial fluid from the bulk solution. For instance, a quantity Θ, related to the phase π will write Θ_π, with $\pi = f, s, b$ for the interstitial fluid, the skeleton and the bulk solution respectively.

The dual nature (fluid or solid) of the continuous medium addressed by poromechanics implies description in both eulerian and lagrangian frames to account for the interstitial solution and the solid skeleton respectively [1]. In the present work we limit our study to the case of small strains at equilibrium, such that no flow of the interstitial fluid is considered and the strain in the skeleton remains small. Under these circumstances, eulerian and lagrangian descriptions become equivalent and thermodynamical quantities are therefore rescaled by the volume of the representative volume element (RVE) of the material at rest.

2.2. Effective pore pressure

Classical poromechanics account separately for the stress related to the skeleton and the one related to the fluid. In a saturated macroporous solid the stress partition is expressed as

$$\begin{aligned} \underline{\underline{\Sigma}} &= (1-\phi)\underline{\underline{\Sigma}}_s + \phi\underline{\underline{\Sigma}}_f \\ &= (1-\phi)\underline{\underline{\Sigma}}_s - \phi P_b \underline{\underline{\mathbb{1}}} \end{aligned} \tag{1}$$

where $\underline{\underline{\Sigma}}$ is the global stress tensor related to the porous continuum, $\underline{\underline{\Sigma}}_s$ and $\underline{\underline{\Sigma}}_f$ are the skeleton and fluid stress tensors respectively, ϕ is the porosity accessible to the fluid (ratio of the total volume of connected pores to the apparent volume of the porous solid) and P_b is the bulk fluid pressure. Thus, the intrinsic averaged stress within the fluid is addressed through the spherical tensor $-P_b\underline{\underline{\mathbb{1}}}$. This comes down to consider that the fluid applies a pressure on the pores walls, which equals the bulk pressure. This assumption is valid in the context of macroporous materials, in which the interstitial fluid pressure is well defined and equal to the bulk fluid pressure as no confinement effect occur. In the case of microporous materials,

except very specific ideal pore geometries (such as slit pores [15, 16, 17]), determination of the fluid pressure in micropores is ambiguous. For instance, this is evidenced by molecular simulations of fluid adsorption on reconstructed models of microporous materials as diverse as porous carbons [18], microporous zeolites [19] and Carbide Derived Carbons [20], which clearly show that only a few number of fluid molecules can fit in the same micropore (as few as one fluid molecule per pore). Consecutively, at the scale of a single micropore, macroscopic thermodynamical quantities such as the pore pressure are ill-defined.

In order to tackle the mechanical effect of the interstitial fluid on the isotropic microporous skeleton, we therefore do not to rely on a local nanoscale description of the material. Instead we consider the material at the RVE mesoscale, at which the number of interstitial fluid molecules is large enough to define the thermodynamical potentials of the fluid. Let G_f be the Gibbs free energy (defined per unit RVE volume) of the interstitial fluid obtained from the thermodynamical identity

$$G_f = \Psi_f + W_f \tag{2}$$

in which Ψ_f is the Helmholtz free energy of the fluid and W_f is the mechanical work generated by the fluid. To estimate the effective mechanical stress related to the mechanical work produced by the fluid, we introduce a mesoscale *effective pore pressure* P_f, defined as the conjugate thermodynamical variable of the porosity as follows

$$W_f = \phi P_f \,. \tag{3}$$

We therefore assumes that, *on average*, the confined fluid behaves like a bulk fluid with a pressure different from that of the external reservoir. In other words, we consider the reservoir and the interstitial fluids as two distinct bulk fluid phases in equilibrium, with different pressures and densities. We emphasize that this assumption is not true in general as it disregards the contribution of the solid/fluid interactions to the energy of the confined interstitial fluid. As a consequence, we show in the following that the difference between the bulk pressure and the effective pressure only results from the difference in density between the two solutions. In a later section of this paper, we discuss the implications of this assumption as well as the limitations of our approach.

The stress partition is thus modified to account for the effective pore pressure

$$\underline{\Sigma} = (1-\phi)\underline{\Sigma}_s - \phi P_f \underline{\mathbb{1}}. \tag{4}$$

The choice of a simple spherical tensor for the effective pore pressure is supported by numerous studies, which demonstrate that the sorption induced strains in microporous solids are isotropic as long as the material structure is isotropic [3, 5, 6, 12]. At the local pore scale, molecular simulations performed with simple pore shapes also show that no deviatoric contribution to the local pressure tensor should be expected [21]. In the following, we show how to relate this effective pore pressure to the relevant parameters of the problem.

2.3. Thermodynamical equilibrium condition of the fluid phase

Let us now consider a microporous solid immersed in an adiabatic and infinitely rigid container filled with a mass m of fluid. In such conditions, the system {skeleton; interstitial fluid; bulk fluid} is an isolated thermodynamic system. In the limit of reversible transformations, the incremental Helmholtz free energy (per unit RVE volume) of the open thermodynamic system {skeleton; interstitial fluid} reads [e.g. 1, Ch. 3]

$$d\Psi = \underline{\Sigma} : d\underline{\Delta} + \mu_f dm_f - SdT. \tag{5}$$

where $\underline{\Delta}$ is the strain tensor, μ_f is the specific chemical potential of the interstitial fluid, m_f is the mass of interstitial fluid, T is the temperature, S and Ψ are the global entropy and global Helmholtz free energy of the porous medium {skeleton; interstitial fluid} respectively. The right hand terms in equation (5) identify the three different ways to exchange energy with the system: mechanical stress, fluid transport or heat transfer. This expression of the skeleton free energy variation is identical to the one encountered in standard poromechanics. Nevertheless, in the case of the microporous solid, the difference with standard poromechanics lies in the expression of the chemical potential, which differs from that of the bulk fluid:

$$\mu_f = \frac{G_f}{m_f} = \psi_f + \frac{P_f}{\rho_f} \tag{6}$$

in which $\psi_f = \Psi_f/m_f$ and $\rho_f = m_f/\phi$ are the specific Helmholtz free energy and the average density of the interstitial fluid respectively. The differential of the Helmholtz free energy of the bulk fluid writes as

$$d\Psi_b = -P_b d\phi_b + \mu_b dm_b - S_b dT \tag{7}$$

in which ϕ_b is the ratio of the volume occupied by the bulk fluid (*i.e* the volume of the container minus the apparent volume of the porous solid) to the volume of the container. In addition, μ_b, m_b and S_b are the chemical potential, the mass and the entropy of the bulk fluid respectively. The conservation of the total fluid mass $m_t = m_f + m_b$ in the isolated system implies $dm_f = -dm_b$. Therefore, (7) may be rearranged as

$$d\Psi_b = -P_b d\phi_b - \mu_b dm_f - S_b dT. \tag{8}$$

The isolated system reaches thermodynamical equilibrium when the global Helmholtz free energy of the system, $\Psi_t = \Psi + \Psi_b$ is minimal, which implies

$$\frac{\partial \Psi_t}{\partial m_f} = \frac{\partial \Psi}{\partial m_f} + \frac{\partial \Psi_b}{\partial m_f} = 0. \tag{9}$$

Using the relations (5) and (8), we can express the thermodynamical equilibrium condition that must be satisfied by the fluid phase:

$$\mu_f = \mu_b. \tag{10}$$

Therefore, we recover the classical thermodynamical equilibrium condition, that is the bulk solution is in chemical equilibrium with the interstitial fluid.

2.4. Constitutive equation of the effective pore pressure

The Gibbs-Duhem equation applied to the bulk and interstitial fluids gives

$$d\mu_b = \frac{dP_b}{\rho_b} - s_b dT \tag{11}$$

$$d\mu_f = \frac{dP_f}{\rho_f} - s_f dT \tag{12}$$

where s_b and s_f are the specific entropy of the bulk fluid and interstitial fluid respectively. Now, let m_{ex} be the excess mass of intersitital fluid defined as follows

$$m_{\text{ex}} = m_f - \rho_b \phi \,. \tag{13}$$

Thus m_{ex} is defined as the difference between the total mass of interstitial fluid and the mass of fluid that would fit in the porous space if the interstitial fluid had the same density as the bulk. Recalling that $m_f = \rho_f \phi$, we obtain

$$\frac{\rho_b}{\rho_f} = 1 - \chi \,, \tag{14}$$

in which the parameter $\chi = m_{\text{ex}}/m_f$ is referred to as the *confinement degree* of the interstitial fluid. The confinement degree equals zero if the interstitial and bulk fluids have identical density and approaches the value 1 if the density of the bulk solution is negligible compared to that of the interstitial fluid. Using the above definition we can rearrange the expression of the incremental chemical potential of the interstitial solution in terms of the confinement degree:

$$d\mu_f = (1-\chi)\frac{dP_f}{\rho_b} - s_f dT \,. \tag{15}$$

Accounting for the thermodynamical equilibrium condition and therefore equating equations (11) and (15), we find the constitutive equation of the effective pore pressure and interaction entropy in its incremental form

$$dP_f - \left(\frac{1}{1-\chi}\right) dP_b - \left(\frac{\rho_b \Delta s}{1-\chi}\right) dT = 0. \tag{16}$$

where $\Delta s = s_f - s_b$ is the specific entropy jump between the interstitial and bulk fluids. Relation (16) relates the quantities resulting from adsorption and confinement of the fluid molecules, $(P_f \,;\, \Delta s)$, to macroscopic quantities $(P_b \,;\, T \,;\, \phi \,;\, \chi)$. In the limit of isothermal transformations, the incremental constitutive equation reduces to

$$dP_f = \frac{dP_b}{1-\chi} \,. \tag{17}$$

The ratio $1/(1-\chi)$ is greater than unity if the confinement degree is larger than zero. Consecutively, the more the interstitial fluid is confined, the higher the effective pore pressure. Intuitively, this prediction is consistent with the experimental observation of the adsorption induced swelling of isotropic microporous materials. Indeed, the swelling should result from an effective pore pressure larger than the bulk fluid pressure.

2.5. Effect on the volumetric strain

In reversible and isothermal conditions, the differential of the Helmholtz free energy of the microporous skeleton is

$$d\Psi_s = \underline{\Sigma} : d\underline{\underline{\Delta}} + P_f d\phi. \tag{18}$$

Classically, in the limit of a linear poroelastic (reversible) behavior, the constitutive equations read [e.g. 1, Ch. 4]

$$\Sigma_{ij} = \frac{\partial \Psi_s}{\partial \Delta_{ij}} = \left\{(K + b^2 N)\epsilon - bN(\phi - \phi_o)\right\}\delta_{ij} + 2Ge_{ij} \tag{19}$$

$$P_f = \frac{\partial \Psi_s}{\partial \phi} = -bN\epsilon + N(\phi - \phi_o) \tag{20}$$

where $\Delta_{ij} = e_{ij} + (\epsilon/3)\,\delta_{ij}$, ϕ_o is the porosity of the material at rest, K is the apparent bulk modulus, G the shear modulus, b and N the Biot coefficient and modulus respectively. Consider now that the microporous solid is placed in a container filled with a fluid at bulk pressure P_b. As a result, the stress tensor $\underline{\Sigma}$ reduces to the hydrostatic bulk pressure acting on the skeleton:

$$\underline{\Sigma} = -P_b \underline{\underline{\mathbb{1}}}. \tag{21}$$

Moreover, by considering the solid matrix to be homogeneous, the Biot coefficient and Biot modulus are related to the apparent bulk modulus K, to the bulk modulus of the material composing the skeleton matrix K_s, and to the porosity at rest ϕ_o as follows:

$$b = 1 - \frac{K}{K_s} \tag{22}$$

$$N = \frac{K_s}{1 - \frac{K}{K_s} - \phi_o} \tag{23}$$

By using the above relations and the constitutive equation of the effective pore pressure (17), equations (19) and (20), in their incremental forms, yield the volumetric deformation and porosity increments, denoted as $d\epsilon$ and $d\phi$ respectively, as functions of the increment of bulk pressure:

$$d\epsilon = \left\{\left(1 - \frac{K}{K_s}\right)(1-\chi)^{-1} - 1\right\}\frac{dP_b}{K} \tag{24}$$

$$d\phi = \left(1 - \frac{K}{K_s} - \phi_o\right)(1-\chi)^{-1}\frac{dP_b}{K_s} + \left(1 - \frac{K}{K_s}\right)d\epsilon. \tag{25}$$

The swelling strain ϵ is obtained by summation of $d\epsilon$ between P_{b0} and P_b:

$$\epsilon - \epsilon_0 = \int_{P_{b0}}^{P_b} \frac{dP_b}{K}\left\{\left(1 - \frac{K}{K_s}\right)(1-\chi)^{-1} - 1\right\} \tag{26}$$

The microporous material swells for positive values of $d\epsilon$, which leads to the following swelling condition:

$$\chi > \frac{K}{K_s}\,. \tag{27}$$

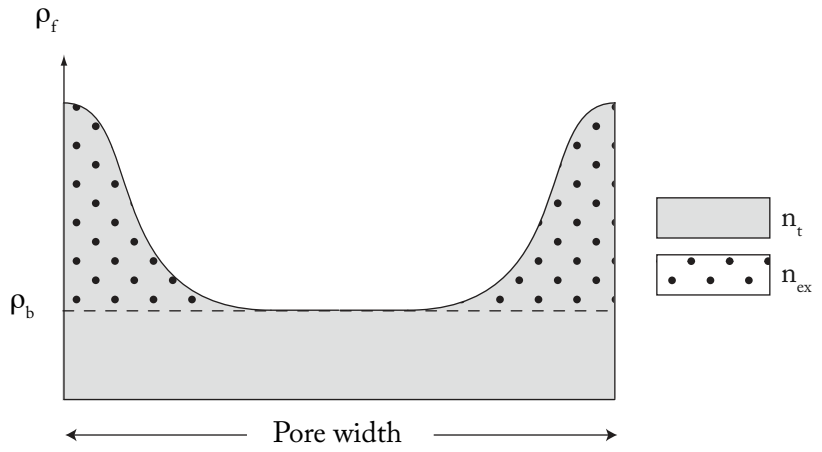

Figure 1: Sketch of the fluid density profile in a micropore. The gray colored area stands for the total number of interstitial fluid n_{t} present in the pore. The dotted area stands for the excess quantity of interstitial fluid which corresponds to the excess number of moles n_{ex} of the Gibbs adsorption isotherm.

Thus, according to our model, the microporous medium should swell all the more so as the interstitial fluid is highly confined and the porous skeleton exhibits low K/K_s ratios. On the other hand, due to the compression of the skeleton matrix, shrinkage should occur if

$$\chi < \frac{K}{K_s}\,. \tag{28}$$

This might be the case for materials exhibiting a high K/K_s ratio (materials with a high proportion of occluded porosity) along with negligible fluid confinement.

3. Adsorption induced swelling of saturated isotropic microporous materials

In this section, we show how the effective pore pressure and the swelling strains may be deduced from adsorption measurements. Since coal is a multi-scale porous material, our model is only relevant to the microporous part of this material. However, several experiments performed on centimeter-wide microporous coal specimen can be found in the literature, in which the samples do not exhibit any meso/macroporosity that would result from natural cracks [4, 5, 6]. We therefore compare the theoretical predictions of the model with these specific sets of experimental data.

3.1. Relating the effective pore pressure to adsorption data

Most experimental studies of gas sorption on porous materials focus on the measurement of the Gibbs adsorption isotherm [22]. As shown in Figure 1, the Gibbs adsorption isotherm stands as a measurement of the number n_{ex} of adsorbate moles that exceeds the number of

fluid moles at bulk conditions. Let n_{t} be the total number of moles of interstitial fluid (see Figure 1). Then the confinement degree of the interstitial fluid may be expressed as

$$\chi = n_{\mathrm{ex}}/n_{\mathrm{t}}\,. \tag{29}$$

However, adsorption experiments do not provide the total number of moles of interstitial fluid contained in the porous adsorbent during sorption. From the experimental point of view the excess number of moles adsorbed is indeed the only measurable quantity. Nevertheless, the total number of interstitial fluid moles can still be estimated from the excess number of moles by assuming that the model correctly predicts the evolution of the porosity. Hence the following relation

$$\begin{aligned} n_{\mathrm{t}} &= n_{\mathrm{ex}} + \frac{\rho_b V_\phi}{M} \\ n_{\mathrm{t}} &= n_{\mathrm{ex}} + \left(\frac{\phi}{1-\phi}\right)\frac{m_s}{M}\frac{\rho_b}{\rho_s} \end{aligned} \tag{30}$$

where V_ϕ is the connected porous volume of the material, M the molar mass of the adsorbed gas, m_s the adsorbent sample mass and ρ_s the density of the material composing the solid matrix of the porous adsorbent. It is obvious, from equation (30), that the confinement degree and the porosity of the material are coupled. Consecutively, we use the incremental equations (24) and (25), coupled with (30), to compute the total number of interstitial fluid moles from excess adsorption isotherm data. For a given set of parameters K, K_s and ϕ_o, we performed the calculation of the volumetric strain and porosity as follows:

- We used the experimental excess adsorption isotherm (P_b , n_{ex}) as input. The number of data points was increased by linear interpolation.
- At $P_b = 0\,\mathrm{MPa}$, the initial strain, porosity and confinement degree were set to $\epsilon(0) = 0$, $\phi(0) = \phi_o$ and $\chi(0) = 0$ respectively.
- At step i, the confinement degree was defined as $\chi(i) = n_{\mathrm{ex}}(i)/n_{\mathrm{t}}(i)$, where $n_{\mathrm{t}}(i)$ was obtained from equation (30) with $\phi = \phi(i)$.
- The strain and porosity of step $i+1$ were obtained as $\epsilon(i+1) = \epsilon(i) + d\epsilon(i)$ and $\phi(i+1) = \phi(i) + d\phi(i)$ respectively. We used equations (24) and (25) with $\chi = \chi(i)$ to compute the strain and porosity increments respectively.

3.2. Comparison with experimental data

3.2.1. Comparison with data from Day et al

Day et al performed adsorption experiments and swelling measurements on several Australian bituminous coals [4, 5] . More specifically, they used digital cameras and a pressure cell equipped with sight windows to measure the swelling strain of a Bowen basin coal sample during sorption of CO_2, at $T = 55°C$ and up to $P_b = 15\,\mathrm{MPa}$ [4]. In addition, they performed CO_2 adsorption isotherms measurements on other Bowen basin coal samples at

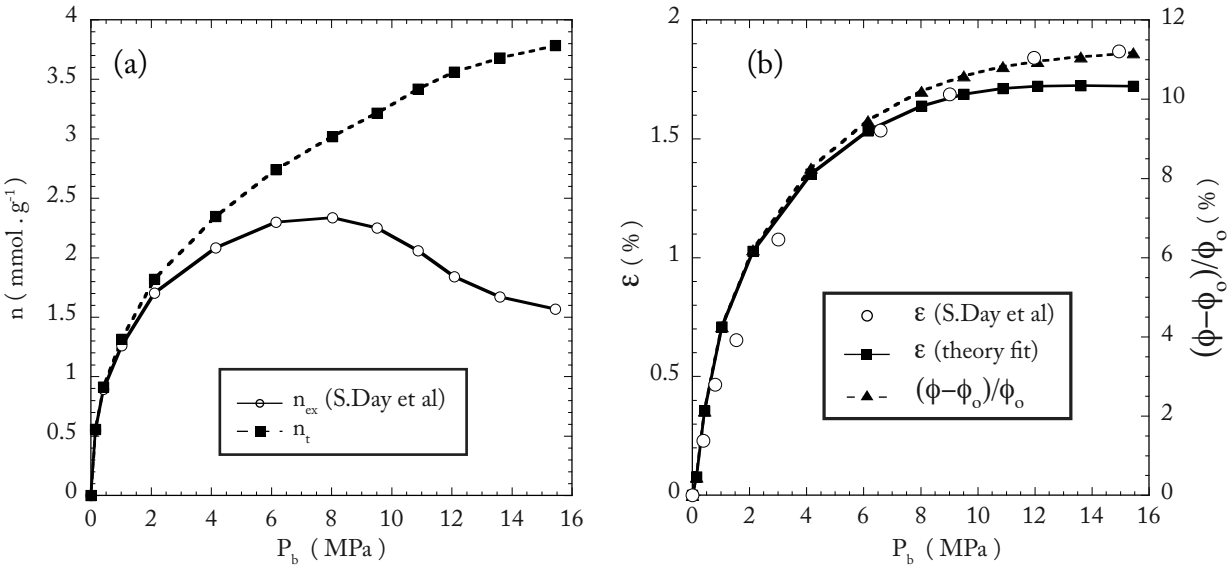

Figure 2: (a) Adsorption isotherm of CO_2 on a Bowen basin coal. White circles stand for the excess adsorption isotherm measured by Day et al [5]. Black squares stand for the total number of moles of interstitial fluid, computed from equation (30) with an initial porosity of $\phi_o = 0.148$. The lines are guides for the eye. (b) Evolution of the swelling strain and porosity with the bulk pressure. White circles stand for the swelling measured by Day et al [4]. The black squares represent the fit of the model prediction with the apparent bulk modulus as the adjustable parameter. The black triangles are the model predictions for the relative variation of porosity. Results read $K = 3.48\,\mathrm{GPa}$. The lines are guides for the eye.

$T = 53°C$ and up to $P_b = 16\,\mathrm{MPa}$ with a gravimetric technique [5]. To compare the theoretical model predictions with the swelling data from [4], we use the adsorption data from [5] corresponding to the Bowen basin coal sample referred to as "Qld 5", whose porosity $\phi_o = 0.148$ was measured by helium pycnometry. In order to limit the number of degrees of freedom of the fitting procedure to only one adjustable parameter, we set the solid matrix bulk modulus to $K_s = 7.6\,\mathrm{GPa}$. This value is consistent with mechanical tests coupled to helium injection performed by Hol and Spiers [23], which are, to our knowledge, the only measurements of the bulk modulus of bituminous coals' solid phase reported in the literature. The volumetric strain is then computed and fitted to the swelling measurements from

Data source	Gas type	m_s (g)	ρ_s $(kg.m^{-3})$	ϕ_o	K (GPa)	K_s (GPa)
Day et al	CO_2	4.1	1358	0.148	3.48*	7.60[a]
Ottiger et al	CO_2	40.81	1265	0.085*	2.65[a]	7.60[a]
Ottiger et al	CH_4	40.81	1265	0.106*	2.65[a]	7.60[a]

$*$ Adjusted. a Assumed.

Table 1: Summary of model parameters for coal swelling

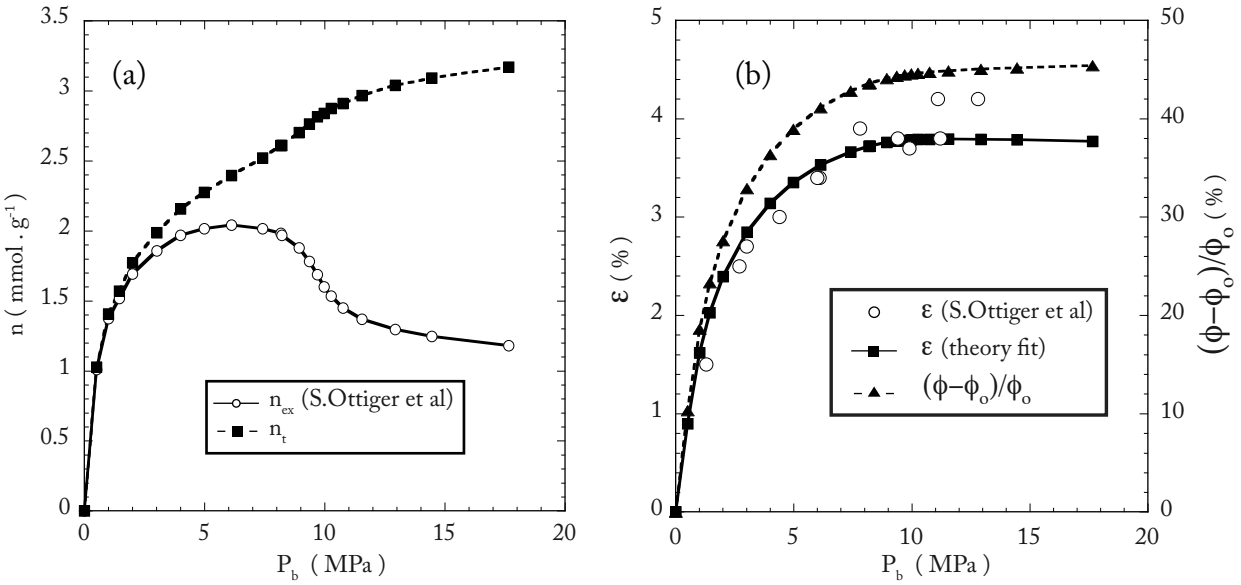

Figure 3: (a)Adsorption isotherm of CO_2 on a Sulcis province coal White circles stand for the excess adsorption isotherm measured by Ottiger et al [6]. Black squares stand for the total number of moles of interstitial fluid, computed from equation (30) with an initial porosity of $\phi_o = 0.0850$. The lines are guides for the eye. (b) Evolution of the swelling strain and porosity with the bulk pressure. White circles stand for the swelling measured by Ottiger et al [6]. The black squares represent the fit of the model prediction with the initial porosity as the adjustable parameter. The black triangles are the model predictions for the relative variation of porosity. Results read $\phi_o = 0.0850$. The lines are guides for the eye.

[4] with K as the only adjustable parameter. Table 1 summarizes the model parameters used in the calculations. Figure 2(a) shows the measured excess adsorption isotherm n_{ex} of CO_2 on the Qld 5 sample as well as the quantity n_{t} deduced from equation (30). Figure 2(b) superposes the experimental strain with the fitting curve obtained for $K = 3.48\,\text{GPa}$. This fitted value falls in the range of the apparent bulk modulus of coals[24, 25] and we observe a good agreement between the swelling strain predicted by the model and experimental data. Moreover, figure 2(b) reports the relative variation of the porosity with bulk pressure. The porosity follows the same trend as the volumetric strain, but with a final increase of almost 11%.

3.2.2. Comparison with data from Ottiger et al

Ottiger et al performed adsorption isotherm measurements of pure CO_2, pure CH_4 and (CO_2, CH_4) mixtures on bituminous coal samples from the Sulcis Province (Italy) at $T = 45°C$ and up to $P_b = 19\,\text{MPa}$, coupling manometric and gravimetric techniques [6]. In addition, they used a pressure cell equipped with sight windows and a digital camera to measure the swelling strain during sorption. In their paper, Ottiger et al do not report any measurement of the coal samples' porosity. In the following we hence fit the model predictions to the swelling data with the initial porosity ϕ_o as the only adjustable parameter

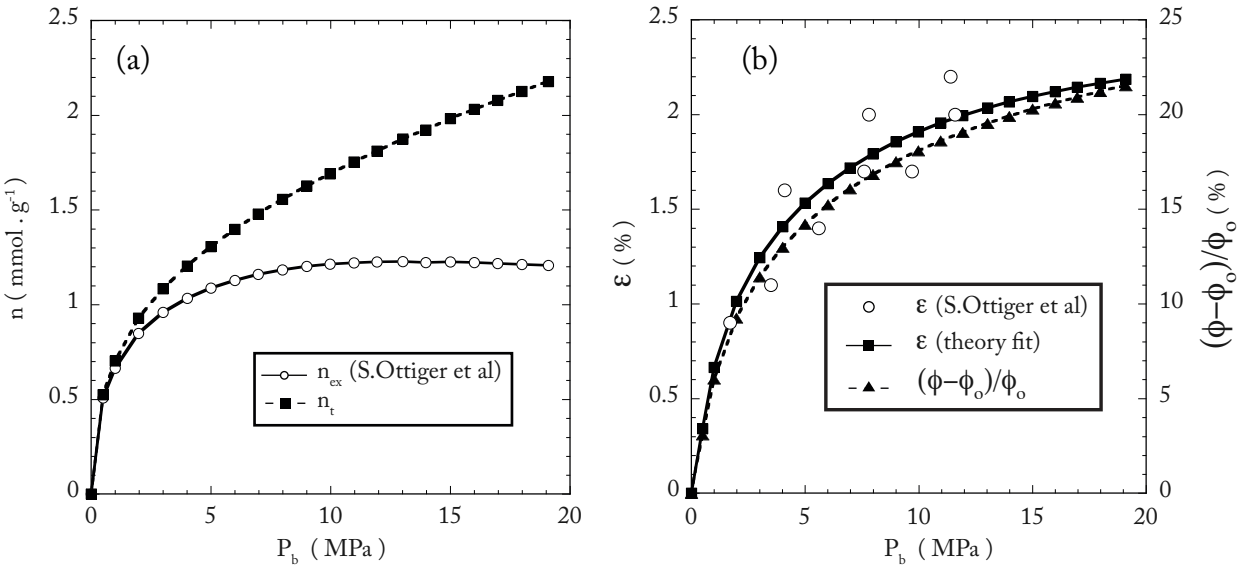

Figure 4: (a)Adsorption isotherm of CH_4 on a Sulcis province coal White circles stand for the excess adsorption isotherm measured by Ottiger et al [6]. Black squares stand for the total number of moles of interstitial fluid, computed from equation (30) with an initial porosity of $\phi_o = 0.1056$. The lines are guides for the eye. (b) Evolution of the swelling strain and porosity with the bulk pressure. White circles stand for the swelling measured by Ottiger et al [6]. The black squares represent the fit of the model prediction with the initial porosity as the adjustable parameter. The black triangles are the model predictions for the relative variation of porosity. Results read $\phi_o = 0.1056$. The lines are guides for the eye.

(cf. table 1). We set the apparent bulk modulus to $K = 2.65\,\mathrm{GPa}$. This value of the apparent bulk modulus, consistent with experimental data found in the literature [24, 25], is the same as Brochard et al obtained by fitting their poromechanical model to Ottiger et al data. We emphasize that we use this specific value in order to directly compare our model to that of Brochard et al in a later section of this paper. The bulk modulus of the solid phase is set to $K_s = 7.60\,\mathrm{GPa}$, as previously. Figures 4 and 3 report the results for pure CO_2 and pure CH_4 respectively. The fitted porosity reads $\phi_o = 0.0850$ in the case of the sorption of pure CO_2, and $\phi_o = 0.1056$ in the case of the sorption of pure CH_4. In both cases, we observe a good agreement between the theoretical predictions and the experimental data. The fitted porosities of $\phi_o = 0.1056$ and $\phi_o = 0.850$ are consistent with the typical values observed for bituminous coals, ranging from 0.04 to 0.18 according to helium pycnometry measurements performed by Day et al [5]. Furthermore, as previously observed, the relative variation of the porosity predicted by the model follows the same trend as the volumetric strain. However, the range of the increase in porosity is one order of magnitude higher than the swelling strain. In particular, the increase in porosity can exceed 45% in the case of CO_2 injection. While the coal sample used in CH_4 and CO_2 swelling experiments is the same, the porosity obtained for CH_4 differs from that obtained for CO_2 by 19%. Ottiger et al did

not perform the adsorption measurements on the same coal sample as the one they used for the swelling measurements. Other studies point out that the adsorption isotherms of CH_4 and CO_2 on two different coal samples may substantially differ, even if these samples belong to the same coal bed [3, 6]. As the computed strains depend directly on the adsorption isotherms, this might explain the discrepancy observed between the two porosity values.

4. Discussion

4.1. Helmholtz free energy and entropy jumps

The Helmholtz free energy jump $\Delta\psi$ is defined as the difference between the specific Helmholtz free energies of the interstitial and bulk fluids when the system reaches equilibrium. If we consider isothermal transformations, the free energy jump reads

$$\Delta\psi = \frac{P_b}{\rho_b} - \frac{P_f}{\rho_f} \tag{31}$$

It follows from equations (17) and (31) that the sign of the free energy jump is therefore given by the following function F:

$$F(P_b) = f(P_b)P_b - \int_0^{P_b} dP_b f(P_b) \tag{32}$$

in which f is the function defined as

$$f(P_b) = (1 - n_{\text{ex}}/n_{\text{t}})^{-1}. \tag{33}$$

The function F is always negative if the function f monotonically decreases with P_b. The derivative of f with respect to P_b reads

$$\frac{df}{dP_b} = (1 - n_{\text{ex}}/n_{\text{t}})^{-2} \frac{d}{dP_b}\left(\frac{n_{\text{ex}}}{n_{\text{t}}}\right). \tag{34}$$

Experimental data found in the literature and reported in figures $2(a)$, $3(a)$ and $4(a)$ clearly show that the ratio $n_{\text{ex}}/n_{\text{t}}$ decreases with P_b. Consequently, we deduce from equation (34) that f is a monotonic decreasing function of P_b and thus F is negative. As a result, the free energy jump is negative as well and we find:

$$\psi_f - \psi_b = \Delta\psi \leq 0. \tag{35}$$

Therefore, because of the confinement in the micropores, the interstitial fluid cedes free energy to the skeleton under the form of mechanical work, which provokes the swelling phenomenon. When adsorption and confinement effects become negligible, the ratio $n_{\text{ex}}/n_{\text{t}}$ tends to 0 and so does the free energy jump. In such conditions, the interstitial and bulk fluid specific Helmholtz free energies are equal.

Now, let us focus on the sign of the entropy jump Δs in the general case of non-isothermal transformations. By rearranging equation (16), we obtain

$$\Delta s = \frac{1}{\rho_b}\left((1-\chi)\frac{dP_f}{dT} - \frac{dP_b}{dT}\right). \tag{36}$$

Several experimental studies point out that the swelling strain, as well as the adsorbed excess number of fluid molecules, decrease upon increasing the temperature ([6], [26]). If we consider the paradigm of §2.3, these results suggest that the effective pore pressure P_f and the number of bulk fluid moles in the external bulk solution, n_b, decreases and increases respectively with temperature ($dP_f/dT \leq 0$ and $dn_b/dT \geq 0$). Moreover, in the case of small swelling strain, the volume V_b occupied by the external bulk fluid (i.e the volume of the fluid container minus the volume of the porous solid) does not significantly vary upon swelling ($dV_b \simeq 0$). Consecutively, assuming the bulk fluid behaves as an ideal gas, the derivative of the bulk fluid pressure with respect to temperature reads

$$\frac{dP_b}{dT} \simeq \frac{Rn_b}{V_b} + \frac{RT}{V_b}\frac{dn_b}{dT}. \tag{37}$$

In such conditions, the bulk fluid pressure increase with temperature ($dP_b/dT \geq 0$). Therefore, considering the above remarks and the expression of the entropy jump (36), we find:

$$s_f - s_b = \Delta s \leq 0. \tag{38}$$

This result makes sense as the order in the interstitial fluid increases due to the confinement of the fluid molecules in the micropores, and consecutively, the increase of the average fluid density. When adsorption and confinement effects become negligible, the quantities $1-\chi$ and P_f/P_b asymptotically tends to unity. In these conditions, equation (36) shows that the entropy jump vanishes.

4.2. Comparison with the previous study by Pijaudier-Cabot et al

In a previous study, Pijaudier-Cabot et al developed a simplified poromechanical model to address fluid adsorption and confinement effects in microporous materials [15]. In the limit of isothermal reversible transformations, and accounting for the thermodynamical equilibrium condition, the free energy balance of the porous solid reads

$$d\Psi_s = \underline{\Sigma} : d\underline{\Delta} + P_b d\phi^* - d\Psi_{\text{int}} \tag{39}$$

where Ψ_{int} is an interaction energy and ϕ^* is a corrected porosity defined as $\phi^* = \phi/(1-\chi)$. Although the approach is quite similar to the present study, the effective pore pressure is not introduced in this formulation. The interaction energy Ψ_{int} is directly related to the actual pore pressure at the pore scale, which is not well defined. As a consequence, direct calculation of the interaction energy is impossible and further assumptions are thus required. More specifically, the interaction energy is set as a function of the corrected porosity ϕ^* only, and consecutively an interaction pressure P_{int} is defined as:

$$P_{\text{int}} = \frac{\partial \Psi_{\text{int}}}{\partial \phi^*} \tag{40}$$

In the equation of state of the microporous solids, this interaction pressure plays exactly the same role as the effective pore pressure introduced in the present work. A prototype constitutive equation is introduced:

$$P_{\text{int}} = -k\, n_{\text{ex}} \tag{41}$$

where k is a proportionality constant. This empirical constitutive relation is based on the experimental observation of Levine, who pointed out the relation of proportionality between the Gibbs adsorption isotherm and the swelling strain of coal at low bulk pressures [3]. Nevertheless, according to experimental datas from Ottiger et al [6] and Day et al [4, 5], this approximation breaks down at high bulk pressure, as the swelling strain is monotonic whereas the Gibbs adsorption isotherm reaches a maximum and then decreases (see figures 2 and 3). Therefore, the knowledge of the adsorbed excess number of moles n_{ex} is not sufficient to accurately predict the effective pressure that induces the swelling.

4.3. Comparison with the work of Brochard et al

Recently, Brochard et al proposed a reformulation of poromechanics to account for adsorption induced stress in microporous solids [12, 13]. Although their approach is quite similar to the present work, the main difference lies in the fact that they do not account for the solid and fluid phases separately. Indeed, their model is based on the energy balance of the porous medium (solid and fluid) considered as a whole, as opposed to the model developed in the present paper, which introduces the porosity of the material. As a consequence, although their model does not provide any information about the variation of porosity, it is however laid down in more general perspectives because it does not imply any assumption regarding the interaction between the solid and the interstitial fluid. With the notations of the present paper, the hydrostatic stress obtained by Brochard et al reads

$$\sigma = K\epsilon - \frac{\partial}{\partial \epsilon}\left[\int_0^{P_b} N_t \bar{V_b} dP_b\right]_{P_b}, \tag{42}$$

where N_t is the number of moles of interstitial fluid per unit RVE volume, and $\bar{V_b}$ is the molar volume of the bulk reference fluid. By recalling that $1 - \chi = N_b/N_t$, where $N_b = N_t - N_{ex}$ is defined as the number of moles of interstitial fluid that would fit in the porous volume at bulk density, the hydrostatic stress obtained with the present model is:

$$\sigma = K\epsilon - b\int_0^{P_b} \frac{N_t}{N_b} dP_b. \tag{43}$$

By noting that the bulk molar volume is a function of the pressure only, and that, per definition, $\phi = N_b\bar{V_b}$ and $b = [\partial\phi/\partial\epsilon]_{P_b}$, the two models are equivalent provided the following equation holds:

$$\left[\frac{\partial N_t}{\partial \epsilon}\right]_{P_b} = \left[\frac{\partial \phi}{\partial \epsilon}\right]_{P_b} \frac{N_t}{\phi} \tag{44}$$

Therefore, the models are compatible if the quantity of interstitial fluid is proportional to the porosity. Under such condition $[\partial N_t/\partial\phi]_{P_b} = N_t/\phi$ and equation (44) is correct. In other

words, the two models can be considered to be equivalent if, on average, the interstitial fluid behaves like a bulk fluid, which is the central assumption of our model. Furthermore, Brochard et al compared their model predictions to Ottiger et al experimental data. To do so, they assumed that the quantity of interstitial fluid depends linearly on the volumetric strain, which is implicit in equation (44). They hence define a so-called multivariate adsorption isotherm as follows,

$$N_t(\epsilon, P_b) = N_t^o(P_b)(1 + C(P_b)\epsilon) \tag{45}$$

where $C(P_b)$ is defined as a coupling coefficient. Upon inserting the above adsorption isotherm in the constitutive equations (42) and (43), and then by equating those two equations, we obtain the following expression for the coupling coefficient:

$$C(P_b) = \frac{b}{\phi - b\epsilon} \tag{46}$$

In table 2, we report the values of $C(P_b)$ adjusted to Ottiger et al data, obtained by Brochard et al and from equation (46) respectively. Values of the parameters required for the calculation of $C(P_b)$ from equation (46) are listed in table 1. In particular, the apparent bulk modulus of coal is set to $K = 2.65\,\mathrm{GPa}$, which is the same value as reported by Brochard et al. We observe a good agreement between the two models. This suggests that the underlying assumption of our model is reasonable in the context of supercritical fluid adsorption in amorphous microporous solids such as coal.

Gas type	$C(P_b)$, Brochard et al	$C(P_b)$, this work
CO_2	$7.60 \pm 20\%$	$6.89 \pm 8\%$
CH_4	$6.05 \pm 7\%$	$5.92 \pm 2\%$

Table 2: Quantitative comparison with the model of Brochard et al based on a fit of Ottiger et al data.

4.4. Limitations of the model

As discussed previously, the central assumption of our model consists in considering that, on average, the interstitial fluid behaves like a bulk fluid with pressure P_f. This assumption is not true in general because it neglects the contribution of solid/fluid interactions to the energy of the interstitial fluid. For instance, when dealing with ideal micropores models (slit, cylindrical or spherical pores), the solid/fluid interactions result in a strong structural ordering of the confined fluid and thus drive its thermodynamical state. More specifically, in the case of slit pores models, these interactions induce the organization of the fluid in one or several layers parallel to the planar pore walls. This layering results in a so-called solvation (or disjoining) pressure highly sensitive to the distance between the solid planes and therefore sensitive to the porosity [15, 16, 27, 28]. This pressure can be positive or negative and is thus conducive to swelling or shrinkage of the microporous material. At the scale of the RVE, such effects are significant in crystalline microporous solids with well-defined pores' geometries and narrow pore size distributions: under such conditions structural effects in the confined

fluid are indeed important and local mechanisms involved at the pore scale directly impact the global behavior of the material [29]. Shrinkage may also occur in isotropic microporous materials, as evidenced by experiments performed on carbide derived carbons by Yakovlev et al [30]. Our model, in its present formulation, cannot reproduce the shrinkage strains observed in these experiments. Several factors should however reduce these confinement induced ordering effects and the possible resulting shrinkage: (1) temperature, because it increases molecular disorder; (2) Roughness of the pore walls, because it kills the symmetry of the pore structure; (3) Polydispersity and isotropy of the porous network, because local mechanisms are more likely to compensate at the scale of the RVE. For instance, Yakovlev et al observed that increasing the temperature suppress the adsorption-induced shrinkage and then only monotonous swelling is observed. In addition, Brochard et al performed molecular simulations of gas sorption on unidimensional elastic carbon chains [12] . Their results show that shrinkage is observed for crystalline chains, whereas amorphous chains can only swell. Therefore, we arguably consider that our model pertains to amorphous microporous solids with broad pore size distribution under high temperature conditions.

5. Conclusion

We have shown that the poromechanical theory can be refined to account for adsorption induced swelling in saturated isotropic microporous solids. Because of fluid adsorption and confinement effects in the micropores, the interstitial fluid is likely to exchange mechanical work with the microporous skeleton, which eventually leads to the swelling of the porous solid. The introduction of an effective pore pressure allows us to infer the virtual pressure jump between the bulk and interstitial solutions, without relying on the description of the interstitial fluid state at the local pore scale. By accounting for the chemical equilibrium of the fluid phase, the effective pore pressure is related to a reduced set of macroscopic variables. This work explicitly quantifies the influence of the fluid molecules confinement degree on the volumetric deformation of isotropic microporous solids during sorption of fluid. In particular, this study points out the dependency of the effective pore pressure, and consecutively the swelling strain and porosity variation, on the ratio between the excess number of adsorbed moles n_{ex} and the total number of interstitial fluid moles n_{t}. We have observed a fair agreement between the fit of the theoretical predictions and several sets of experimental data found in the literature. In addition, the significant variation of porosity, as predicted by the model, suggests that the adsorption-induced swelling is likely to impact fluid transport mechanisms through the microporous network.

Acknowledgements: Financial supports from ERC advanced Grant project Failflow (Ad-G 27769) is gratefully acknowledged.

References

[1] O. Coussy, Poromechanics, John Wiley Pubs, 2004.
[2] O. Coussy, Mechanics and Physics of Porous Solids, John Wiley Pubs, 2010.

[3] J. R. Levine, Model study of the influence of matrix shrinkage on absolute permeability of coal bed reservoirs, Geol. Soc. Spec. Pub. 109 (1996) 197–212.
[4] S. Day, R. Fry, R. Sakurovs, Swelling of australian coals in supercritical CO_2, url = http://linkinghub.elsevier.com/retrieve/pii/S0166516207001334, volume = 74, year = 2008, Int. J. Coal Geol. (????) 41–52.
[5] S. Day, G. Duffy, R. Sakurovs, S. Weir, Effect of coal properties on CO_2 sorption capacity under supercritical conditions, Int. J. Greenh. Gas Con. 2 (2008) 342–352.
[6] S. Ottiger, R. Pini, G. Storti, M. Mazzotti, Competitive adsorption equilibria of CO_2 and CH_4 on a dry coal, Adsorption 14 (2008) 539–556.
[7] F. Meehan, The expansion of charcoal on sorption of carbon dioxide, Proc. R. Soc. A 115 (1927) 199–207.
[8] D. Bangham, N. Fakhroury, The expansion of charcoal accompagnying sorption of gases and vapours, Nature 122 (1928) 681–682.
[9] M. Vandamme, L. Brochard, B. Lecampion, O. Coussy, Adsorption and strain: The CO_2 - induced swelling of coal, J. Mech. Phys. Solids 58 (2010) 1489–105.
[10] Z. Pan, L. Connell, A theoretical model for gas adsorption-induced coal swelling, Int. J. Coal Geol. 69 (2007) 243–252.
[11] S. Mushrif, A. Rey, An integrated model for adsorption-induced strain in microporous solids, Chem. Eng. Sci. 64 (2009) 4744–4753.
[12] L. Brochard, M. Vandamme, R.-M. Pellenq, Poromechanics of microporous media, J. Mech. Phys. Solids 60 (2012) 606–622.
[13] L. Brochard, M. Vandamme, R. J.-M. Pellenq, T. Fen-Chong, Adsorption-induced deformation of microporous materials: Coal swelling induced by CO_2 - CH_4 competitive adsorption, Langmuir 28 (2012) 2659–2670.
[14] A. Boţan, R. Vermorel, F.-J. Ulm, R. J.-M. Pellenq, Molecular simulations of supercritical fluid permeation through disordered microporous carbons, Langmuir (2013) doi: 10.1021/la402087r.
[15] G. Pijaudier-Cabot, R. Vermorel, C. Miqueu, B. Mendiboure, Revisiting poromechanics in the context of microporous materials, C.R. Mecanique 339 (2011) 770 – 778.
[16] K. Yang, X. Lu, Y. Lin, A. V. Neimark, Deformation of Coal Induced by Methane Adsorption at Geological Conditions, Energ. Fuel. 24 (2010) 5955–5964.
[17] B. D. Todd, D. J. Evans, P. J. Daivis, Pressure tensor for inhomogeneous fluids, Phys. Rev. E 52 (1995) 1627–1638.
[18] J. Pikunic, C. Clinard, C. N., K. Gubbins, J.-M. Guet, R.-M. Pellenq, I. Rannou, J.-N. Rouzaud, Structural modeling of porous carbons: constrained reverse monte carlo method, Langmuir 19 (2003) 8565–8582.
[19] B. Coasne, J. Haines, C. Levelut, O. Cambon, M. Santoro, F. Gorelli, G. Garbarino, Enhanced mechanical strength of zeolites by adsorption of guest molecules, Phys. Chem. Chem. Phys. 13 (2011) 20096–20099.
[20] J. Palmer, A. Llobet, S.-H. Yeon, J. Fischer, Y. Shi, Y. Gogotsi, K. Gubbins, Modeling the structural evolution of carbide-derived carbons using quenched molecular dynamics, Carbon 48 (2010) 1116–1123.
[21] Y. Long, M. Sliwinska-Bartkowiak, H. Drozdowski, M. Kempinski, K. A. Phillips, J. C. Palmer, K. E. Gubbins, High pressure effect in nanoporous carbon materials: Effects of pore geometry, Colloids and Surfaces A: Physicochemical and Engineering Aspects (2012).
[22] F. Rouquerol, J. Rouquerol, K. Sing, Adsorption by powders and porous solids, Academic Press, 1999.
[23] S. Hol, C. J. Spiers, Competition between adsorption-induced swelling and elastic compression of coal at CO_2 pressures up to 100 MPa, Journal of the Mechanics and Physics of Solids 60 (2012) 1862 – 1882.
[24] Z. Zheng, M. Khodaverdian, J. D. Mclennan, Static and dynamic testing of coal specimens, in: 1991 SCA Conference, 9120.
[25] T. Gentzis, N. Deisman, R. Chalaturnyk, Geomechanical properties and permeability of coals from the foothills and mountain regions of western canada, Int J. Coal Geol. 69 (2007) 153–164.
[26] E. Battistutta, P. van Hemert, M. Lutynski, H. Bruining, K.-H. Wolf, Swelling and sorption experiments

on methane, nitrogen and carbon dioxide on dry Selar Cornish coal, Int. J. Coal Geol. 84 (2010) 39–48.
[27] G. Gor, A. Neimark, Adsorption-induced deformation of mesoporous solids, Langmuir 26 (2010) 13021–13027.
[28] P. Kowalczyk, A. Ciach, A. V. Neimark, Adsorption-induced deformation of microporous carbons: pore size distribution effect., Langmuir 24 (2008) 6603–6608.
[29] A. V. Neimark, F.-X. Coudert, A. Boutin, A. H. Fuchs, Stress-based model for the breathing of metal-organic frameworks, The Journal of Physical Chemistry Letters 1 (2010) 445–449.
[30] V. Y. Yakovlev, A. A. Fomkin, A. V. Tvardovski, Adsorption and deformation phenomena at interaction of N_2 and microporous carbon adsorbent., J. Colloid. Interf. Sci. 280 (2004) 305–308.